Self-organized oscillations of strongly coupled dust Coulomb clusters in plasma traps

Yuh-Chyi Wang, Wen-Tau Juan, and Lin I
Department of Physics and Center for Complex Systems, National Central University, Chungli, Taiwan 32054, Republic of China
(Received 25 February 2000)

The self-organized oscillation of a strongly coupled dust Coulomb cluster with an elongated cross section in a weakly ionized rectangular plasma trap is investigated. Through an inverse supercritical bifurcation at the low rf power end, a low-frequency (about 5 Hz) limit cycle oscillation of the whole cluster associated with the intracluster compressional lattice wave and phase-locked oscillation of the glow intensity distribution is observed. It is caused by the interplay of the dust motion and the shrinking and expanding of the confining dark space.

PACS number(s): 52.90.+z, 05.45.−a, 73.23.−b

Self-organized coherent structures and oscillations exist in various nonlinear dissipative extended systems under a continuous input of energy to overcome dissipation [1]. The partially ionized glow discharge consisting of electrons, ions, and neutrals under a constant supply of discharge power is one of the good examples. The ionization, diffusion, and other space-charge-induced transport lead to various interesting self-organized coherent phenomena [2–6]. In this work, we report an experimental observation of the autonomous limit cycle oscillation in a different mesocopic dusty plasma system. The system consists of a strongly coupled small dust Coulomb cluster suspended in a rectangular rf plasma trap.

Recently, the formation of dust Coulomb clusters up to a few hundred dust particles has been demonstrated experimentally [7]. In a small rf glow discharge trap, the dust particles are charged and confined in the center glow region with a quite uniform plasma density, which is surrounded by the dark space (sheath) region with strong outward space-charge field adjacent to the wall of the small confinement cell [7]. The negatively charged dust particles ($\sim 10^4$ electrons per μm-sized dust particle) form a strongly coupled system [8]. Namely, the dust Coulomb cluster is the small dust particle number limit of the large volume Coulomb crystals and liquids studied recently in dusty plasma systems [9,10]. From the condensed-matter physics point of view, it provides a good opportunity to test the generic microscopic structure and dynamical behaviors of the finite-body Wigner crystals or liquids [11]. On the other hand, dust particles in this mesoscopic system do not only interact with each other in a frozen confining background as proposed in many Coulomb cluster models [11]. The interplay with the background plasma could lead to interesting self-organized collective excitations.

In the past few years, self-organized excitations have been observed in several large volume dusty plasma systems. For example, a low-frequency (12 Hz) macroscopic mode with wavelength about 0.5 cm was reported in our strongly coupled rf discharge system [12]. A low-frequency wave with similar frequency (15 Hz) and wavelength (0.6 cm) was observed in the plasma column near the anode disk of a Q-machine with 5-μm dust particles [13]. It was suggested that the fluctuations were a dust acoustic mode. Another recent experiment with 0.1-μm dust particles in an rf discharge system demonstrated the formation of the low-frequency (10 Hz) macroscopic filamentary mode and great void mode [14]. The dust acoustic wave and the ionization wave have been suggested to interpret these two modes, respectively. In addition, ion flow has been used to interpret the cause for driving oscillations, especially around the sheath region where the flow is strong [15].

In a weakly ionized steady-state rf discharge system, electrons and ions are constantly generated through ionization by electrons which mainly gain energy from the external rf power source. Since the electron mobility is higher than the ion, an outward dc space-charge field in the dark space (sheath) surrounding the glow is induced. It balances the rates of electron and ion losses to the wall, and reaches the steady-state condition [16]. The sheath thickness decreases with increasing electron density and electric field. The unfrozen ionization process is quite similar to the reaction in a chemical system and is controlled by the electron density and energy [5]. It plays a positive feedback for varying electron density and sheath thickness, and is responsible for generating self-organized waves and patterns in many dust-free glow discharge systems [3–6].

In our experiment, dust particles are negatively charged and suspended in the glow region. The small cluster has a large surface surrounded by the dark space which has strong electric field and nonuniform electron density distribution. The presence of particles alters the background plasma properties through Coulomb interaction (e.g., electron expelling) and charging-discharging [7], especially when charge fluctuations on dust particles are allowed [17,18]. New collective modes with a slow time scale involving dust motions are expected. In addition to the ion flow effect mentioned above, the unfrozen ionization could also be a possible feedback channel to pump energy from the external rf power source, enhance plasma density and sheath thickness fluctuations, and excite new collective modes. In this work, through tuning the control parameter to a proper window, a supercritical bifurcation to the state with a few Hz phase-locked limit cycle collective oscillations (about the same as the dust plasma frequency) of the cigar-shaped cluster along the major axis of the rectangular confining cell is observed. The oscillation is accompanied by a phase-locked oscillation of plasma emission intensity distribution and a longitudinal acoustic wave traveling along the major axis of the cluster.

The experiment is conducted in a cylindrical rf glow discharge system with 9-cm diameter and 4.5-cm height. Instead of the small circular confinement cell for the circular clusters in our previous experiment [10], a rectangular confining cell with 14.5-mm width, 30-mm length, and 14-mm height is placed at the center of the bottom electrode surface for confining the elongated cluster. Seven μm diameter polystyrene particles are dropped into the weakly ionized glow discharge ($n_i \sim 10^9$ cm^{-3}) generated in 250 mTorr Ar using a 14-MHz rf power system. The rf power system consists of a power amplifier with 50-dB gain, which is driven by a function generator operated at 14 MHz. The output amplitude $V_{\rm rf}$ of the function generator can be digitally controlled (rf power $\propto V_{\rm rf}^2$). Decreasing the rf power increases the dark space thickness surrounding the uniform glow, where a strong outward space-charge field can be supported to confine dust particles with 330-μm interparticle spacing in the center cigar-shaped glow region. Vertically, particles stay in the lower part of the glow. It forms a virtual cathode and induces strong vertical ion winds which vertically align the dusts through the induced dipole-dipole interactions. It enables the convenient viewing of the dust motion on the horizontal plane through an optical microscope connected to the digital video system with a 30-Hz frame rate.

In our experiment, the glow is first loaded with dust particles at a few watt rf power. As the rf power gradually decreases, the dark space thickness gradually increases. It decreases the horizontal cross section of the glow where dusts are confined. The micrograph in Fig. 1(a) shows a snapshot of the top view particle image in the horizontal plane right before the onset of the cluster oscillation at $V_{\rm rf} = 73.05$ mV. The cluster has an elongated shape and is in the cold liquid state with slightly disordered triangular packing. Most of the particles have six nearest neighbors in the horizontal plane. The plasma emission intensity [see the emission contours in Fig. 2(a)] gradually diminishes from the cluster boundary toward the confining cell. The intensity of the emission from the electron impact excited atoms is roughly proportional to the local electron density. The shape of the cluster and the emission intensity contours in Figs. 1(a) and 2(a) show good mirror symmetry with respect to the two axes of the rectangular confining cell. As $V_{\rm rf}$ decreases further, the whole cluster starts to oscillate left and right collectively, through an inverse supercritical bifurcation process. Figure 1(b) shows the sequential snapshots of the cluster oscillation in about one oscillation cycle at $V_{\rm rf} = 72.70$ mV. The glow intensity distribution [Fig. 2(b)] no longer has the reflection symmetry. It also oscillates back and forth along the major axis and phase-leads the cluster oscillation. The higher-intensity side is always accompanied by a thinner dark space.

The upper two sets of curves in Fig. 3(a) show the typical wave forms of the emission intensity $I_{r,l}$ taken from the two points each with 1 mm×1 mm area located at ± 7 mm, respectively, along the major axis from the center of the confining cell [marked by point A and B in Fig. 2(a)] at different $V_{\rm rf}$. The associated lower two sets of curves with more scattered data points correspond to the evolution of the locations $X_{r,l}$ of the rightmost and the leftmost edges of the cluster taken from each image frame. The higher (lower) emission intensity corresponds to the higher (lower) electron density in the narrower (wider) dark space. Note that the instrumentation errors for $I_{r,l}$ and $X_{r,l}$ are 2% of the oscillating amplitude and 0.1 mm, respectively. In order to see the

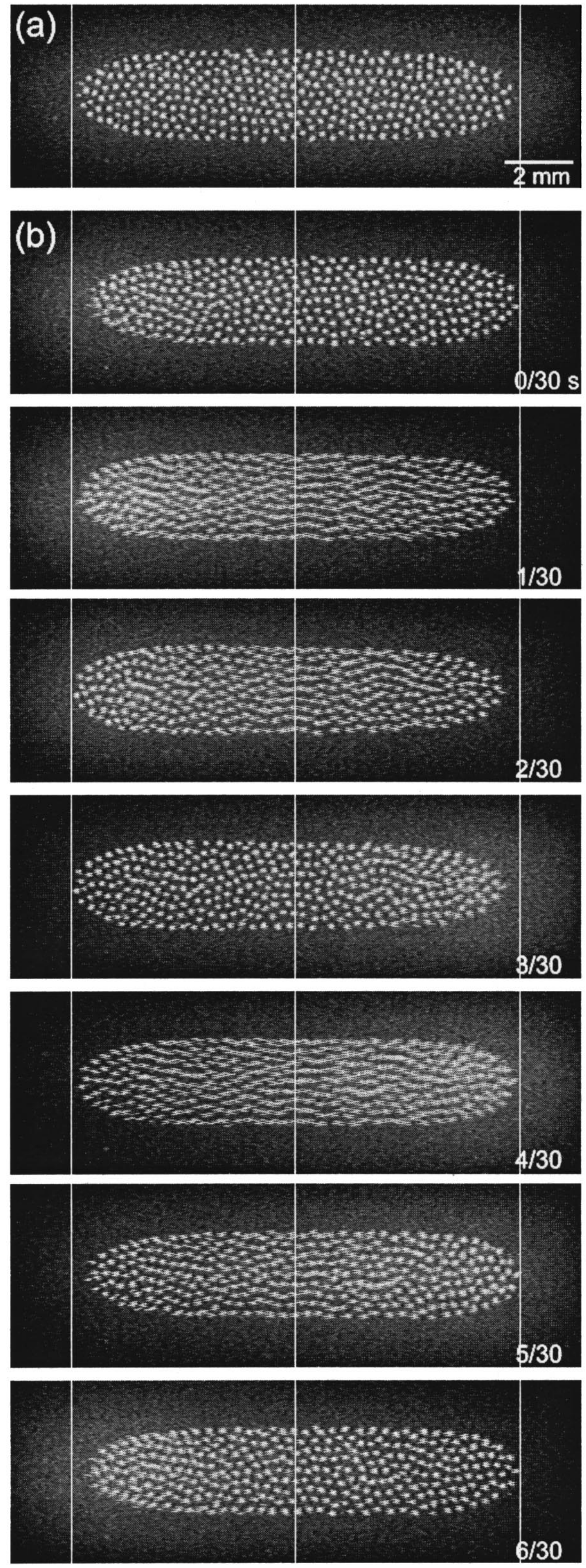

FIG. 1. (a) The top view of the cluster illuminated by a horizontal laser sheet before the onset of the autonomous oscillation at $V_{\rm rf} = 73.05$ mV. The surrounding region shows the symmetric glow. (b) The sequential snapshots with 30 Hz sampling rate and 15 msec exposure time show the typical oscillation of the cluster associated with the intracluster compressional wave and the phase-lead oscillation of the glow at $V_{\rm rf} = 72.70$ mV. The vertical lines are used as guiding references to illustrate the cluster oscillation.

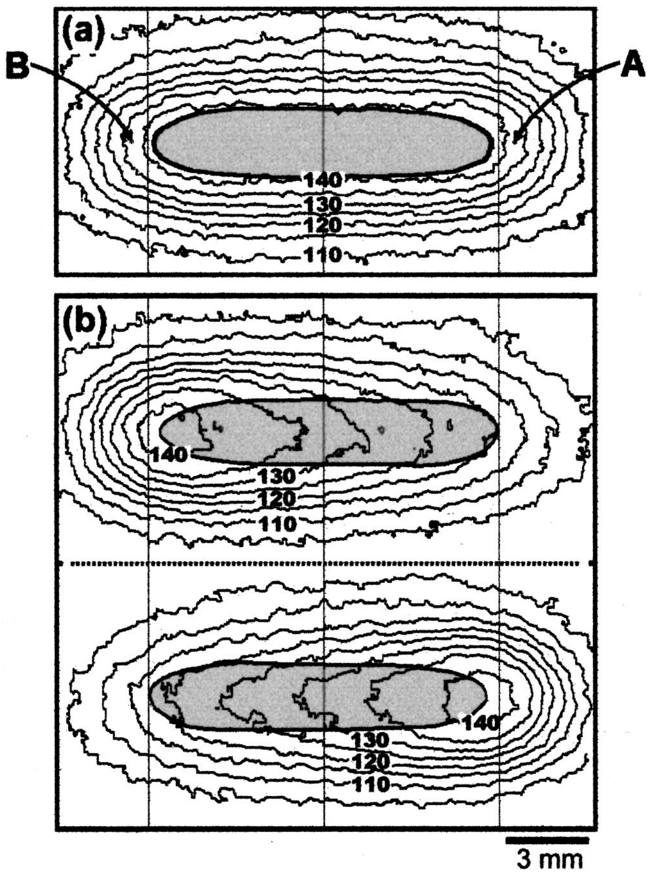

FIG. 2. (a) The snapshot showing the contours of the emission intensity distribution and the relative position of the cluster (the gray area) before the oscillation at $V_{\mathrm{rf}}=73.05$ mV. (b) The two typical snapshots corresponding to the pictures shown at 0 and 0.1 s, respectively, in Fig. 1(b), when the cluster oscillates to the rightmost and the leftmost ends. The motion of the cluster to one end causes the expansion of the dark space around that end.

detailed structure of the wave form from the data under the low sampling rate (30 Hz, i.e., about six points per oscillation cycle), each wave form is reconstructed. We reset the time $t_n = n\Delta t$ for frame n in each time series (with 1000 points) through $t_n' = t_n - NT$ such that $0 < t_n' < 3T$. $\Delta t = \frac{1}{30}$ s and N is a varying integer. T is the oscillation period which can be obtained by slowly scanning it until all the data points of $I_{r,l}$ converge on a simple periodic wave form. The small scattering of the data points of $I_{r,l}$ indicates that the intensity oscillations have stable amplitude and frequency. The oscillations of I_r and I_l are 180° out of phase. $X_{r,l}$ also show phase-locked periodic oscillation with respect to $I_{r,l}$. For example, X_r decreases (the cluster moves leftward) after I_r decreases (the right dark space expands). In Fig. 1 (e.g., the fourth picture), the particle speeds (i.e., $\propto$ length of the trajectory) are modulated through the cluster. It manifests a long-wavelength compressional wave associated with the oscillation of the center of mass of the cluster. The data points of $X_{r,l}$ are more scattered than those of $I_{r,l}$, due to the complication by the compressional wave.

The wave form and the frequency of the limit cycle oscillation change with the decreasing rf power. Right after the onset of the oscillation ($V_{\mathrm{rf}}=72.70$ mV), there is a 5.28-Hz peak in the power spectrum [Fig. 3(b)]. As V_{rf} decreases to 71.30 mV, the amplitude increases. The frequency also increases to 5.38 Hz [Fig. 3(b)]. The wave forms become more nonsinusoidal and the corresponding phase portraits constructed from the delayed time series of $I_r(t_n)$ shown in Fig. 4(a) also become less symmetric due to the more nonlinear motion [19]. Figure 4(b) shows the bifurcation diagram. The motion also causes the breaking of the mirror symmetry of the cluster shape about the short axis. For example, pushing and pulling by the expanding and shrinking dark space can make the leading side of the cluster fatter than the opposite side.

Our system belongs to the general category of the nonequilibrium steady-state nonlinear systems. The self-organized limit-cycle-type oscillation usually occurs through bifurcation when the feedback with proper phase and strength can overcome the system damping. Our negatively charged dust cluster is confined by the space-charged field adjacent to the confining trap. In a frozen space-charge background without feedback and nonlinear processes, a perturbed cluster should return to its center equilibrium position through the damped oscillation at dust plasma frequency (damped by the neutral gas through friction). In our system, the electron-ion generation, transport, and loss processes are not frozen. They could be the possible sources for feeding energy and driving the oscillation. The ion flow toward the sheath has been proposed to be the mechanism for driving the particle motion around the sheath area in other previous

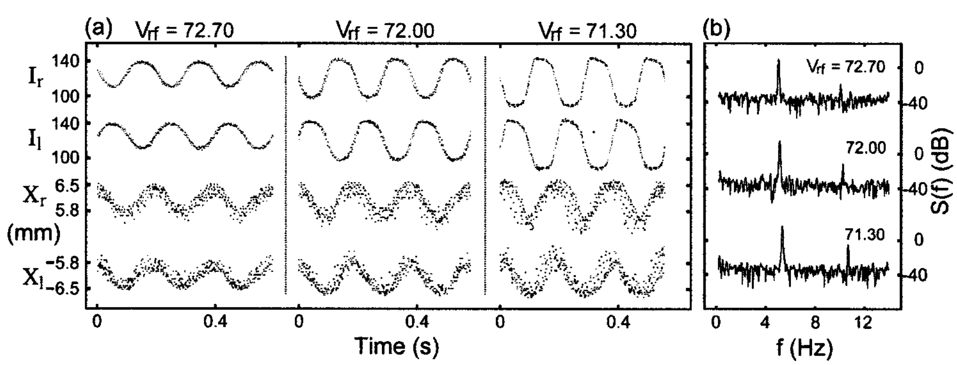

FIG. 3. (a) Upper two sets of curves: the reconstructed wave forms of the glow intensity $I_{r,l}$ taken from the two points located at ± 7 mm from the center of the rectangular cell along the x axis at different V_{rf}. Lower two sets of curves: the reconstructed wave forms of the two edge positions $X_{r,l}$ of the cluster. (b) The power spectra of I_r at the corresponding V_{rf}.

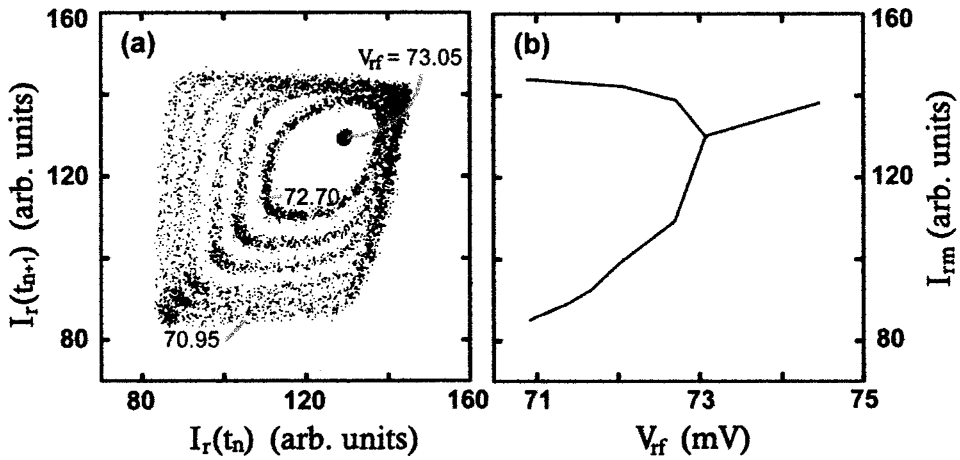

FIG. 4. (a) The reconstructed phase portraits from the delayed time series of $I_r(t_n)$ with $\frac{1}{30}$ sec delay time at different V_{rf} starting from $V_{rf}=73.05$ for the fixed point and then changing with $\Delta V_{rf}=-0.35$ mV for the successive limit cycles. (b) The bifurcation diagram constructed from I_{rm}, the maximum and the minimum values of $I_r(t_n)$ series, as V_{rf} changes.

works [15]. Note that the wave observed in Barken's experiment also propagated along the cathode-anode axis along which ions and electrons flow [13]. However, in our system, the negatively charged dust particles stay in the lower part of the glow under the gravitational force. They form a virtual cathode and attract large vertical ion flow. Ions are mainly flowing vertically downward instead of horizontally. This is evidenced by the vertical alignment of particles induced under the ion flow even when the cluster is under horizontal oscillation. In certain other control parameter windows, the vertical ion flow can indeed induce the vertical oscillation of particles in the lower part of the vertical chains. Nevertheless, it seems that the small horizontal ion flow cannot be a major source for driving the observed horizontal oscillation of the entire cluster.

We would like therefore to propose a mechanism to explain the observed phenomena. The expanding and shrinking sheath under the uneven distribution of rf power may be a more proper source to drive the cluster oscillation. The sheath has a nonuniform electron density distribution. As proposed by Nitter *et al.* [20], the charging on dust particles which move into and out of the sheath could lead to collective particle motion. Nunomura *et al.* used a similar idea with delayed charging and extra neutral gas friction to explain the observed particle oscillation [21]. In our system, the instability occurs at very low rf power where the plasma density is low and very sensitive to the dust density distribution. The observed variation of the emission intensity distribution manifests the phase-locked variation of electron density distribution associated with cluster motion. When the cluster moves toward one end under a small perturbation, the negatively charged dust particles will change the local electron density through sinking or expelling electrons. The situation is reversed at the opposite end. The total input rf power is fixed but could be unevenly distributed depending on the local electron density. Lower (higher) rf power is distributed in the end region with lower (higher) electron density to generate lower (higher) ionization. This feedback further enhances the decrease of electron density and the expansion (shrinking) of the dark space where the space-charge field is weak (strong). It causes the effective pushing and pulling of the cluster by the dark spaces at the two ends, respectively. The situation is reversed when the cluster overshoots to the opposite end due to its large inertia. It leads to the limit cycle oscillation of the cluster if a proper feedback phase is reached. At the low rf power end, the ionization degree is very low. The rf power distribution is more sensitive to the electron density distribution. Therefore, the oscillation has a larger amplitude as rf power decreases. Our system is similar to a damped particle oscillating in a confining well which also rocks at a frequency locked with particle oscillation and gains energy from the external power source.

The finite-body cluster has a finite number of degrees of freedom. The liquid state is not rigid and completely incompressible. The cluster rocking can drive a compressional wave with wavelength about the same order as the cluster size, even though the compressional lattice wave is usually damped in a dissipative dusty plasma system [22]. Namely, a soft collective mode is excited and is associated with the motion of the center of mass of the cluster.

In our system, the dust mass is 1.9×10^{-13} kg and the dust density is 3×10^{10} m^{-3}. The force of gravity on each particle is 1.9×10^{-12} N. Given a plasma potential of 20 V and a sheath thickness of 6 mm, the averaged electric field in the sheath is 3000 V/m. It gives an upper bound about 4000 e per dust to float the dust particle, since dust particles stay inside the sheath region where the electric field is stronger than the averaged field. If we assume the cluster oscillating frequency is close to the dust plasma frequency, the 5-Hz frequency gives $Q\sim1400$ e. It falls in the right range of the dust charges estimated above. Certainly, a more rigorous theory is needed for the observed phenomena. The various processes such as dust charging-discharging, the impact of dust particles on the background plasma density distribution coupled with the unfrozen ionization process, the spatio-temporal variation of plasma sheath, particle transports, etc., should be considered.

In conclusion, we have observed the formation of the self-organized limit cycle oscillation of a small elongated cluster in a rectangular plasma trap through an inverse bifurcation as the rf power decreases. The interplay between the clusters and the background plasma leads to the phased-locked oscillation of the sheath width and revives the damped cluster oscillation around the dust plasma frequency. The dark space forcing also induces the compressional-type lattice waves in the cluster.

This research was supported by the National Science Council of the Republic of China under Contract No. NSC-88-2112-M008-008.

[1] See, e.g., A.V. Gaponov-Grekhov, *Nonlinearities in Action* (Springer, Berlin, 1992); M.C. Cross and P.C. Hohenberg, Rev. Mod. Phys. **65**, 851 (1993); S.H. Strogatz, *Nonlinear Dynamics and Chaos* (Addison-Wesley, Reading, MA, 1994).
[2] Y.P. Raizer, *Gas Discharge Physics* (Springer, Berlin, 1987).
[3] I. Grabec, Phys. Fluids **17**, 1834 (1974).
[4] E. Ammelt, D. Schweng, and H.-G. Purwins, Phys. Lett. A **179**, 348 (1993); I. Muller, E.A. Ammelt, and H.-G. Purwins. Phys. Rev. Lett. **82**, 3428 (1999).
[5] J.H. Chu and Lin I, Phys. Rev. A **39**, 233 (1989); Lin I and J.M. Liu, *ibid.* **46**, R733 (1992); Phys. Rev. Lett. **74**, 3161 (1995).
[6] C.Y. Liu and Lin I, Phys. Rev. E **57**, 3379 (1998).
[7] W.T. Juan, Z.H. Huang, J.W. Hsu, Y.J. Lai, and Lin I, Phys. Rev. E **58**, R6947 (1998); W.T. Juan, J.W. Hsu, Z.H. Huang, Y.J. Lai, and Lin I, Chin. J. Phys. (Taipei) **37**, 184 (1999).
[8] C.K. Goertz, Rev. Geophys. **27**, 271 (1989).
[9] J.H. Chu and Lin I, Phys. Rev. Lett. **72**, 4009 (1994); Lin I, W.T. Juan, and C.H. Chiang, Science **272**, 1626 (1996).
[10] Y. Hayashi and K. Tachibana, Jpn. J. Appl. Phys., Part 1 **33**, 804 (1994); G.E. Thomas *et al.*, Phys. Rev. Lett. **73**, 652 (1994).
[11] See, e.g., J.J. Thomson, Philos. Mag. **39**, 236 (1904); V.M. Bedanov and F.M. Peeters, Phys. Rev. B **49**, 2667 (1994).
[12] J.H. Chu, J.B. Du, and Lin I, J. Phys. D **27**, 296 (1994).
[13] A. Barkan, R.L. Merlino, and N. D'Angelo, Phys. Plasmas **2**, 3563 (1995).
[14] G. Praburam and J. Goree, Phys. Plasmas **3**, 1212 (1996).
[15] See, e.g., V.A. Schweigert *et al.*, Phys. Rev. E **54**, 4155 (1996); Phys. Rev. Lett. **80**, 5345 (1998); F. Melandso, Phys. Rev. E **55**, 7495 (1997).
[16] B. Chapman, *Glow Discharge Processes* (Wiley, New York, 1981).
[17] J.X. Ma and M.Y. Yu, Phys. Plasmas **2**, 1343 (1994).
[18] J.A. Sen and P.K. Kaw, Phys. Scr. **51**, 385 (1995); P.K. Kaw and R. Singh, Phys. Rev. Lett. **79**, 423 (1997).
[19] P. Grassberger and I. Procaccia, Phys. Rev. Lett. **50**, 346 (1983).
[20] T. Nitter, T.K. Aslaksen, F. Melandso, and O. Havnes, IEEE Trans. Plasma Sci. **22**, 159 (1994).
[21] S. Nunomura, *et al.*, Phys. Rev. Lett. **83**, 1970 (1999).
[22] G. Praburam and J. Goree, Phys. Rev. Lett. **77**, 3137 (1996).